



Energy and Exergy Analysis on Modified Closed Wet Cooling Tower in Iraq

Qasim Saleh Mahdi*

Hayder Mohammad Jaffal**

*Department of Mechanical Engineering/ Al-Mustansiriyah University

* Department of Environmental Engineering/ Al-Mustansiriyah University

*E-mail: qasim602006@yahoo.com

**E-mail: hayder.jaffal@yahoo.com

(Received 3 September 2015; accepted 12 January 2016)

Abstract

The present study involves experimental analysis of the modified Closed Wet Cooling Tower (CWCT) based on first and second law of thermodynamics, to gain a deeper knowledge in this important field of engineering in Iraq. For this purpose, a prototype of CWCT optimized by added packing under a heat exchanger was designed, manufactured and tested for cooling capacity of 9 kW. Experiments are conducted to explore the effects of various operational and conformational parameters on the towers thermal performance. In the test section, spray water temperature and both dry bulb temperature and relative humidity of air measured at intermediate points of the heat exchanger and packing. Exergy of water and air were calculated by applying the exergy destruction method on the cooling tower. Experimental results showed a significant performance improvement when using packing on the CWCT. It can be observed that the thermal efficiency for the CWCT with packing under a heat exchanger and CWCT with packing above the heat exchanger are approximately 40% and 25% higher than that of the CWCT without packing respectively. As another part of the experiment results, it is indicated that the exergy destruction is directly proportional to air flow rate, cooling water flow rate, inlet cooling water flow rate and inlet Air Wet Bulb Temperature (AWBT) whereas, it is inversely proportional with spray water flow rate. In comparison with the cooling capacity of the tower, it was found that the exergy destruction approximately less than 20%. Exergy efficiency behavior is inversely proportional with the behavior of the exergy destruction. Empirical correlations are obtained to predict water film heat transfer coefficient and air-water mass transfer coefficient considering the influences of operational parameters.

Keywords: Closed Wet Cooling Tower (CWCT), exergy, packing, thermal performance.

1. Introduction

There are two types of wet cooling towers: open and closed cooling towers. In the open cooling tower, the water is in direct contact with the air at surface of the packing. In conventional CWCTs recirculated water is sprayed over a horizontal tube bundle, while air is drawn over the bundle and the cooling water is circulated in tubes and never contacts the outside air. The advantage of CWCT is the limited of pollution dangers with airborne dusts as well corrosion. It has a wide range of applications in the fields of electrical power, chemical industry and building air conditioning. With more and more closed cooling

tower applications, the study also received increasing attention [1].

Much attention has been paid to issues on CWCTs relating to experimental studies and developed correlations of heat and mass transfer coefficients as a function of operating conditions. Armando & Facao [2], designed a new CWCT in order to examine effects of the operating parameters on the saturation efficiency for a CWCT modified for use with chilled ceilings in buildings. Qureshi & Zubair [3], presented theoretically a thermodynamic analysis of counter flow wet cooling towers and evaporative heat exchangers using both the first and second law of thermodynamics. By applying an exergy balance on each of the systems, the variation of second-

law efficiency as well as exergy destruction as a function of various input parameters such as inlet AWBT & inlet water temperature has been identified. Shim et al. [4&5], investigated experimentally the thermal performance of two heat exchangers in closed-wet cooling tower having a rated capacity of 2 TR. Both heat exchangers have multi path that is consumed as the entrance of cooling water and are consisting of bare-type copper tubes of 15.88 mm and 19.05 mm. Heyns & Kroger [6], investigated the thermal performance characteristics of an evaporative cooler, which consist of 15 tube rows with 38.1 mm outer diameter galvanized steel tubes arranged in a triangular pattern of 76.2 mm. Zheng et al [7], investigated thermal performance of an oval tube CWCT based on heat and mass transfer under different operating conditions. Ramkumar and Ragupathy [8], have been investigated thermal performance of open type mechanical draft counter flow cooling tower with expanded wire mesh packing. Exergy analysis has been applied to study the cooling tower potential of performance using the psychrometric gun technique.

In the relevant literature, no results have been reported so far involving the performance of CWCT with packing. The aim of this research is to evaluate thermal performance of modified CWCT with added packing based on first and second law of thermodynamics in Iraq.

2. Experimental Apparatus and Procedure

2.1. Description of Test Rig

A new counter flow CWCT was designed and constructed in which different operating parameters could be varied and tested in the laboratories of Environmental Engineering Department of Al-Mustansiriyah University, College of Engineering. The general arrangement of the equipment is shown in Figure (1). In general, the apparatus consists essentially of cooling column and three major systems; spray water, cooling water and air blowing. The tower fabricated from galvanized steel sheet to provide

protection from rusting and corrosion, each sheet of 1.5 mm thickness, connected together by screws and nuts as a rectangular box of external dimensions 420 mm in width, 760 mm in depth and 280 mm in height, mounted rigidly on a frame which is welded construction with a channel section at the base welded together from the rectangle.

As exists in every forced cooling, the test section consists of three zones: spray, fill (cooling zone) and rain zone. Spray zone is at a height of 180 mm suitable to ensure water distribution uniformly to all points in the fill section. Fill zone at 1000 mm height and characterized as consisting of three places for sliding removable drawer rectangular boxes at the same dimensions, manufacturing for packing and heat exchangers to ensure change the locations and types of heat exchangers and height of packing to study the influence of all these additions on the performance of the tower. The rectangular drawer made of galvanized steel with dimensions of 420 mm in width, 760 mm in depth and 280 mm in height. Six holes along the side of each (drawer) box were done to measure the water temperature, air dry bulb temperature and air relative humidity. The rain zone at a height of 450 mm in the case of three boxes and it will be variable when lifting one or two packing's and increases as decreases the packing height. Air from the atmosphere, enters the single stage centrifugal blower at a rate which is controlled by the butterfly valve. The fan discharges into the PVC pipe and the entrance duct before entering the packed column. As the air flows through the packing and heat exchanger, its moisture content increases and the water in the heat exchanger are cooled. Hot water is pumped from the load tank through the control valve and a water flow meter to the heat exchanger placed inside the test section of tower. Plain tube heat exchanger was designed and manufactured for the present work. The tubes were fixed horizontally in test section inside supported frame of rectangular drawer.

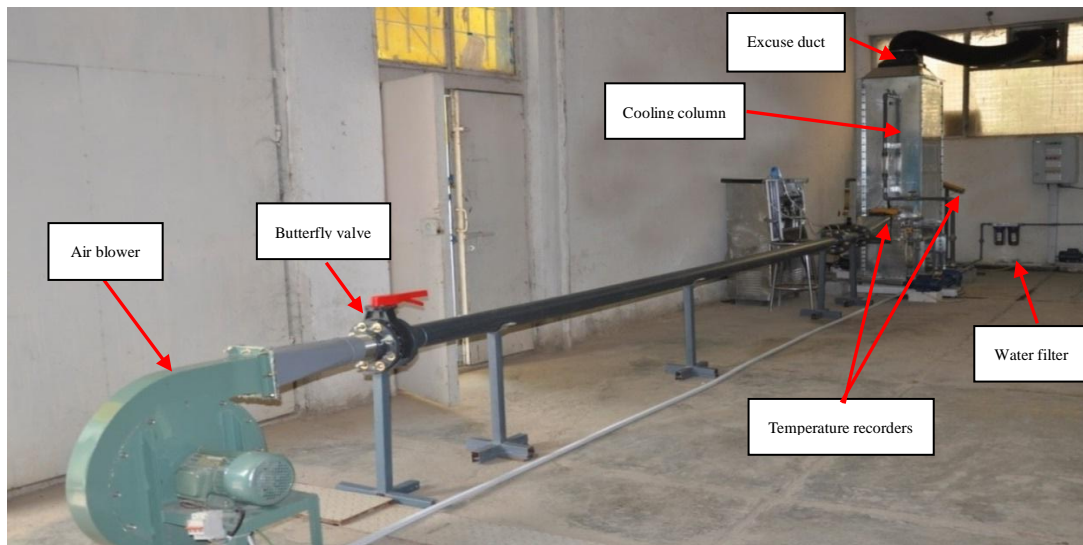


Fig.1. Photographic picture for experimental apparatus (lateral view).

Cooling water moves through the tubes while the spray water and air move over the tubes in perpendicular direction. The tubes are arrayed in staggered arrangement with (equilateral) tube pitch of $3D_o$ (pitch over diameter of 3). The specification of heat exchangers shows in Table (1).

Table 1, Physical dimension of heat exchanger.

Heat exchanger configuration	Value	Unit
Length (L_1)	690	mm
Height (L_2)	166	mm
Width (L_3)	381	mm
Number of tubes for coil	30	-
Vertical tube spacing (X_L)	24	mm
Horizontal tube spacing (X_T)	80	mm
Tube per row	5	-
Outside tube diameter	15.88	mm
Tube thickness	0.81	mm
Total heat transfer area	1032691.77	mm ²
Minimum free flow area	209148	mm ²

The basic geometry for an idealized single pass cross flow tubular (bar type) exchanger with staggered tube arrangement is shown in Figure (2).

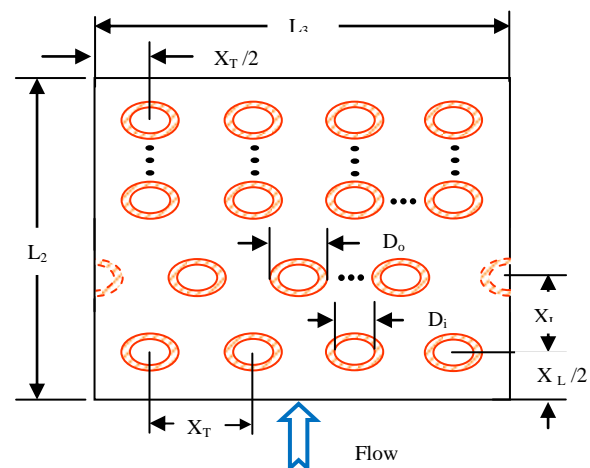


Fig. 2. Tubular single pass exchanger with staggered tubes arrangement [9].

In the present study, 18 sheets with area of ($760 \times 280 \text{ mm}^2$) film type fills consist of vertical corrugated sheets arranged vertically forming an angle relative to one another of 45° viewed in the main direction of flow of the air. The sheets are joined to make rectangle units were fixed in test section inside supported frame of rectangular drawer. For better cooling performance, corrugated film packing were tested in different location arrangement with heat exchanger at a height of 280 mm and 560 mm.

The water distribution system in the cooling tower should distribute the water uniformly over the tube bundle and packing inside the tower, to be the most coefficient method of uniform water distribution in counter flow wet-cooling tower a

pressurized spray system used with different types of spray nozzles. The spray water passes through the spray nozzles and constantly distributed at the upper part of the test section, controlled by means of flow control valve globe type located downstream of the spray water pump. The water distribution system, for the purpose of this study, consists of a spray head (25.4 mm pipe) and six nozzles. The nozzles mounted on branching pipes, of 125 mm each, from the main pipe and the same diameter as the main. The length of the whole arrangement of pipes is 800 mm. The spray head is designed to give two sets of nozzles; each set consists of three nozzles and pointed to a direction opposite to the other set. This would give a net distance of 130 mm between the centres of each two adjacent nozzles. Figure (3) shows the spray nozzles arrangement.



Fig. 3. Spray nozzles arrangement.

2.2. Test Procedure

In order to evaluate the thermal performance of cooling tower, a series of experiments was carried out at different operational and conformational parameters. Operational parameters demonstrate: air flow rate of (0.12-0.3) kg/s, spray water flow rate of (20,25,30,35,40,45) l/min, cooling water flow rate of (10,15,20,25,30,35,40,45,50) l/min, inlet cooling water temperature of (35,40,45,50,55) °C and inlet AWBT of (7-24) °C. Conformational parameters indicate: height of packing used (560) mm, location of packing (under heat exchanger and above heat exchanger).

Thermocouples type K inserted before and after the cooler coil to measure cooling water temperature. To measure the spray water temperatures at intermediate locations inside test section, especially channels have been manufacturing to insert thermocouples through holes. These holes are closed by rubber stoppers through which thermocouples are inserted to measure the temperature profile. The variations of air dry bulb temperature and relative humidity along the test section as well as the inlet and outlet of the tower were measured by humidity meter, which combined temperature/humidity sensor. The humidity meter model TH-305 has a (main faction) temperature and relative humidity measurement range from 0 to 60 °C and 20 to 95% respectively. The sensor probe handle is placed directly in the air stream and connected to display.

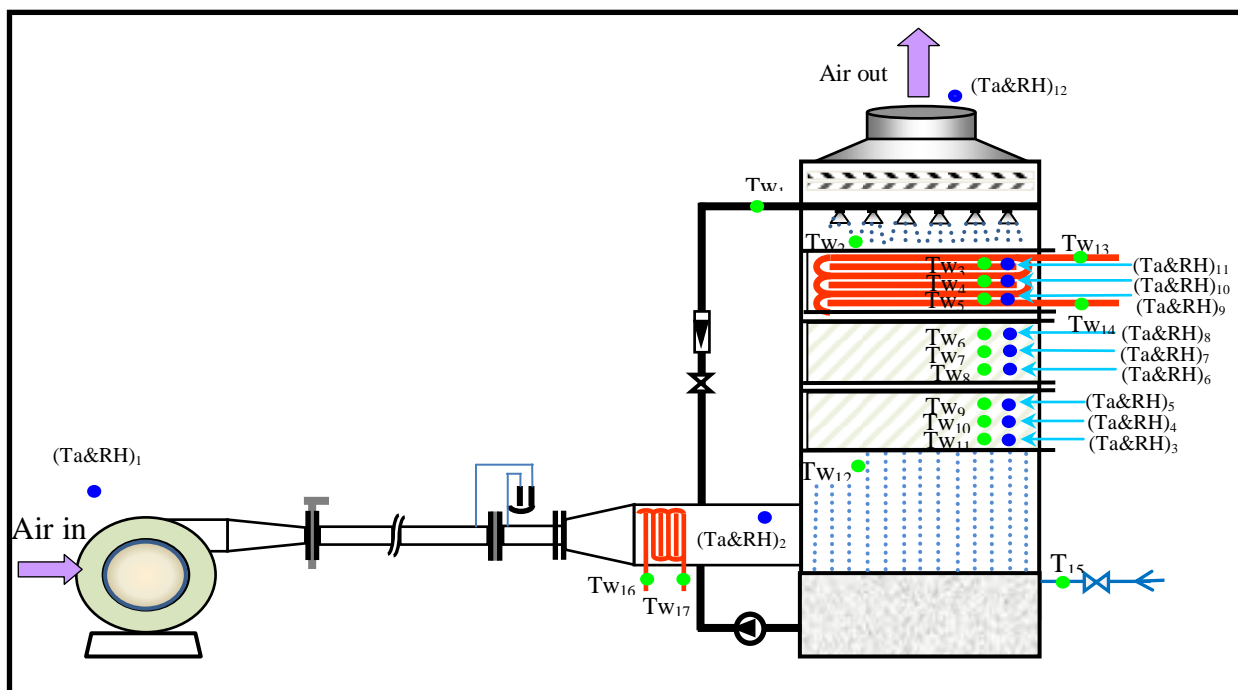


Fig. 4. Locations of thermocouples and humidity meter in the test rig.

2.3. Performance Parameters

2.3.1. Energy Analysis

In viewpoint of energy analysis, the parameters used to determine the performance of cooling tower are:

1- Cooling range: is the temperature difference between the water inlet and exit states. Range can be measured by the temperature difference between the inlet and outlet from cooling tower:

$$CR = T_{cw,in} - T_{cw,out} \quad \dots (1)$$

2- Thermal efficiency: The most important parameter of cooling tower performance is the thermal efficiency, which can be defined as the ratio of actual released of heat to the maximum theoretical heat from cooling tower. The thermal efficiency for the closed circuit cooling towers was defined as [2&10]:

$$\eta = \frac{T_{cw,in} - T_{cw,out}}{T_{cw,in} - T_{awb,in}} \quad \dots (2)$$

3- Cooling capacity: is the heat rejected or heat dissipation, given product of mass flow rate of water, specific heat and temperature difference.

$$q = \dot{m}_{cw} C_{p,cw} CR \quad \dots (3)$$

4-Mass transfer coefficient: The mass transfer coefficient obtained using enthalpy balance for an elementary transfer surface [2].

$$m_a dh_a = \alpha_m (h_i - h_a) dA \quad \dots (4)$$

Which is known as the Merkel equation and integrated for the whole heat exchanger in tower gives:

$$\frac{\alpha_m A}{\dot{m}_a} = \ln \frac{h_i - h_{a,in}}{h_i - h_{a,out}} \quad \dots (5)$$

where, α_m is the mass transfer coefficient for water vapor between spray water film and air, A is the surface area of the heat exchanger and h_i is the specific enthalpy of the saturated air at the mean spray water temperature.

The average of spray water temperatures was taken as the interface temperature according to [7] while the inlet and outlet air enthalpies were calculated from Psychrometric chart according to the measured data. Outlet air enthalpy could be also calculated considering that all the heat goes from water to air [11]

$$\dot{m}_a (h_{a,out} - h_{a,in}) = \dot{m}_{cw} C_{p,cw} (T_{cw,in} - T_{cw,out}) \quad \dots (6)$$

Then the outlet air enthalpy calculates as:

$$h_{a,out} = h_{a,in} + \frac{\dot{m}_{cw} C_{p,cw} (T_{cw,in} - T_{cw,out})}{\dot{m}_a} \quad \dots (7)$$

5-Heat transfer coefficient: Heat transfer from cooling water inside tubes to spray water and air through a water film. the rate of heat transfer from cooling water dq_c is given by [12]:

$$dq_c = \dot{m}_{cw} C_{p,cw} dT_{cw} = -U_o (T_{cw} - T_{sw}) dA \quad \dots (8)$$

Integrated Eq.(8) from the inlet to outlet of cooling water, with constant spray water T_{sw} , gives.

$$\frac{U_o A_c}{C_{p,cw} \dot{m}_{cw}} = \ln \frac{T_{cw,in} - T_{sw,m}}{T_{cw,out} - T_{sw,m}} \quad \dots (9)$$

where, U_o is the overall heat transfer coefficient between cooling water inside the tubes, tube wall and spray water on the outside. It is calculated by the following formula [4]:

$$U_o = \left[\frac{R_o}{R_i} \frac{1}{\alpha_c} + \frac{R_o}{k_t} \ln \frac{R_o}{R_i} + \frac{1}{\alpha_s} \right]^{-1} \quad \dots (10)$$

After the overall heat transfer coefficient was calculated from Eq.(9), it used to calculate, α_s , tube to water film heat transfer coefficient ($W/m^2 C$).

$$\alpha_s = \left[\frac{1}{U_o} - \frac{R_o}{R_i} \frac{1}{\alpha_c} - \frac{R_o}{k_{tube}} \ln \frac{R_o}{R_i} \right]^{-1} \quad \dots (11)$$

Where, α_c is the convection heat transfer coefficient of cooling water inside the tubes, it was calculated by the ‘‘Dittuse-Boelter’’ relation [13]:

$$\alpha_c = 0.023 \frac{k_{cw}}{D_i} Re^{0.8} Pr^{0.3} \quad \dots (12)$$

Where, Reynolds number and Prandtl number were taken for the cooling water inside the tubes.

2.3.2. Exergy Analysis

In this study, the exergy analysis of the CWCT based on the Exergy Destruction Method (EDM) was carried out in the simplified system shown in Figure (5), where the dray air enters the test section from the bottom at the input conditions and crosses the test section at the output conditions while spray water opposed the air direction. On the other hand, cooling water enters the test section inside the heat exchanger perpendicular to the direction of both air and spray water and come out the opposite of entering heat exchanger. For steady state conditions (operating cooling tower), neglecting the effect of kinetic and potential energy, an exergy balance is formulated for all components of the CWCT were presented in Figure (5).

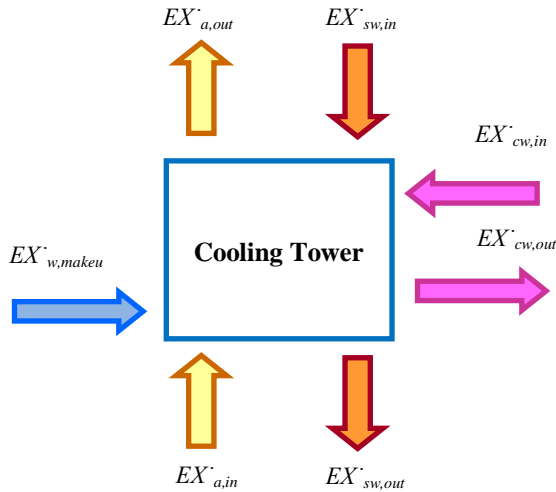


Fig. 5. Exergy balance of the cooling tower.

1-Exrgy of water

Exergy of water can be obtained by Bejan [14]:

$$EX_w^\circ = m_w^\circ [(h_{fw} - h_{fo}) + T_o(S_{fw} - S_{go}) - R_v T_o \ln \phi_o] \dots (13)$$

Neglected the mechanical exergy of water comparing with chemical exergy, so the exergy of water for ideal gas law, Eq. (13) Becomes:

$$EX_w^\circ = m_w^\circ \left[C_{Pw} (T - T_o) - T_o C_{Pw} \ln \frac{T}{T_o} - R_v T_o \ln \phi_o \right] \dots (14)$$

2- Exergy of humid air

The total exergy in the psychrometric process – such as in the cooling tower operating mechanism, without the effect of kinetic and potential energy, on the bases of dray air and water vapour as an ideal gas when neglecting the change of pressure through the cooling tower in the steady state –can thus be generally represented presented in Bejan[14]:

$$EX_a^\circ = m_a^\circ \left[(C_{Pa} + \omega C_{Pv}) \left(T - T_o - T_o \ln \frac{T}{T_o} \right) + R_a T_o \left(1 + 1.608 \omega \right) \ln \frac{1 + 1.608 \omega_o}{1 + 1.608 \omega} + 1.608 \omega \ln \left(\frac{\omega}{\omega_o} \right) \right] \dots (15)$$

3. Exergy Destruction

An exergy balance states that the total exergy increases or decreases within the system boundary

plus the exergy destruction within the same boundary equals the difference between the total exergy transfers in and out across the boundary. Exergy destruction represents by the difference between exergy change of water and exergy change of air.

$$\sum EX_{in}^\circ - \sum EX_{out}^\circ - EX_d^\circ = 0 \dots (16)$$

The exergy destruction can be determined by:

$$EX_d^\circ = (EX_{a,in}^\circ + EX_{sw,in}^\circ + EX_{cw,in}^\circ + EX_{w,makeup}^\circ) - (EX_{a,out}^\circ + EX_{sw,out}^\circ + EX_{cw,out}^\circ) \dots (17)$$

4. Exergy Efficiency

The exergy efficiency (second low efficiency), which is measured of irreversibility losses in a given process is define as [15]:

$$\eta_{Ex} = 1 - \frac{EX_d^\circ}{\sum EX_{in}^\circ} \dots (18)$$

3. Results and Discussions

3.1. Influence of Air and Spray Water Flow Rates

The effect of air flow rate on the cooling capacity for different values of the spray water rate is illustrated in Figure (6). For each value of spray flow rate, as the air flow rate increases; the cooling water range is increases, cooling capacity increased. This can be explained by as the air flow rate increases, rate of evaporated water increases too causing an increasing in the water cooling range. On the other hand, a proportional relation has been shown between the cooling capacity and the spray water flow rate, for the different values of air flow rates. The most important reason for increasing cooling capacity with spray water flow rate is increasing a contact surface for the mass and heat transfer between water and air.

The effect of air flow rate on thermal efficiency for different spray water flow rates illustrated in Figure (7). The cooling tower thermal efficiency increases with the increase of air flow rate and spray water flow rate due to the increase in cooling range and the decrease in tower approach as its calculation from Eq. (3). This behaviour was observed by Yoo et. al. (2010), [16].

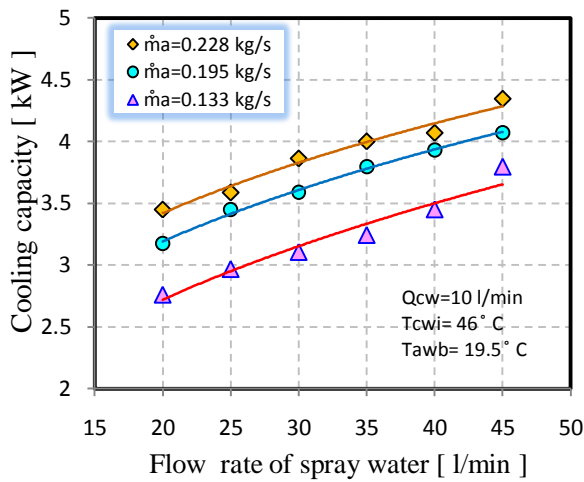


Fig. 6. Variation of cooling capacity with spray water flow rate for different air flow rates.

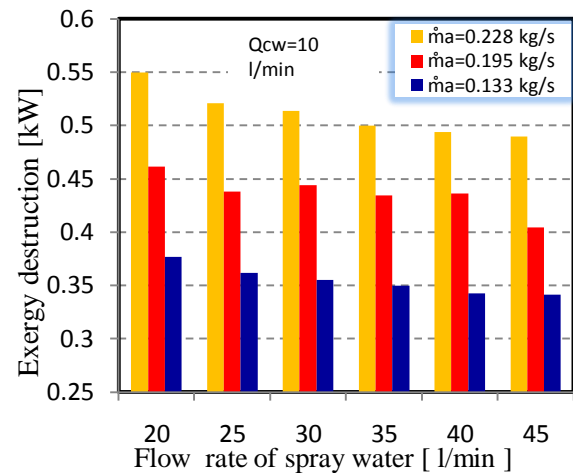


Fig. 8. Variation of exergy destruction with spray water flow rate for different air flow rates.

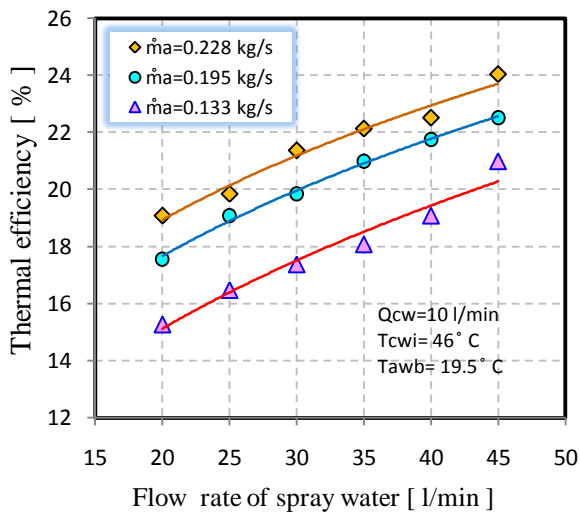


Fig. 7. Variation of thermal efficiency with spray water flow rate for different air flow rates.

The effect of air flow rate on exergy destruction for different spray water flow rates illustrated in Figure (8). Exergy destruction represents by the differences between exergy changes of water and exergy changes of air. For a fixed spray water flow rate, it is observed that the overall cooling tower exergy destruction increases with the increase of the air flow rate due to increase in rate of evaporation losses that causes an increasing in exergy of makeup water. On the other hand, exergy destruction decreases as spray water flow rate increases.

The effect of air flow rate on exergy efficiency for different spray water flow rates illustrated in Figure (9). It is clear that the exergy efficiency inversely proportional to the air flow rate. In other words, exergy efficiency in proportional relation with spray water flow rate.

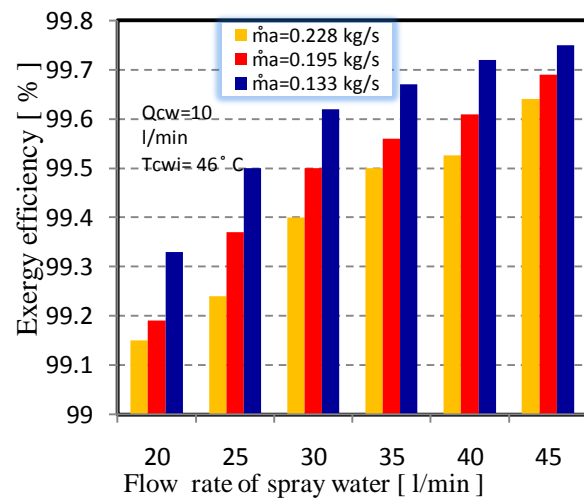


Fig. 9. Variation of exergy efficiency with spray water flow rate for different air flow rates.

Figure (10) shows total exergy change distribution of water and air with the spray water flow rate. Both exergies increases slightly with the increase of spray water flow rate. As indicated in Figure (10), the increasing of spray water flow rate generates an enthalpy increase lead to an increase in exergy of water. The total exergy of air is sum of convection air exergy and evaporation air exergy. Also, it is indicated that the difference

between total exergy change of water and air increases with increasing in spray water flow rate.

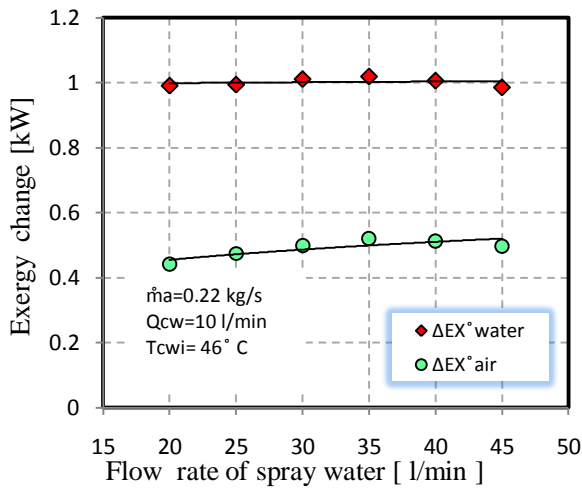


Fig. 10. Variation of total exergy change of water and air with spray water flow rate.

3.2. Influence of Cooling Water Flow Rate

The cooling capacity of tower versus cooling water flow rate with different spray water flow rates is shown in Figure (11). It can be noticed that the cooling capacity is proportional with cooling and spray water flow rates. For each spray water flow rates, cooling capacity increases significantly to increase in cooling water flow rate according to Eq. (3).

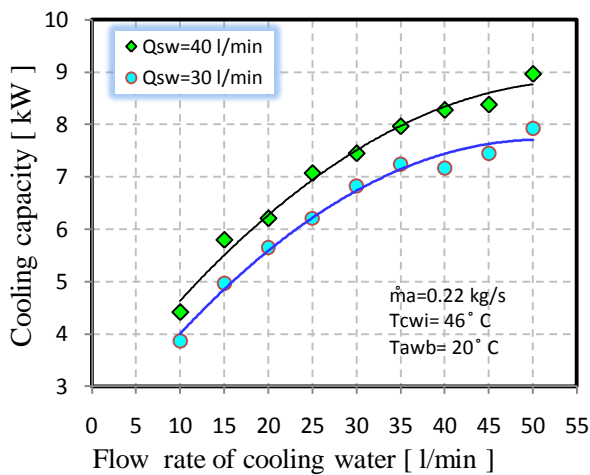


Fig. 11. Variation of cooling capacity with cooling water flow rate for different spray water flow rates.

The effect of cooling water flow rate on thermal efficiency for different spray water flow rates illustrated in Figure (12). Thermal efficiency is inversely proportional to the cooling water flow

rate. At low cooling water flow rate, the opportunity to be the largest in completion of heat exchange caused an increasing in temperature difference of cooling water and thermal efficiency.

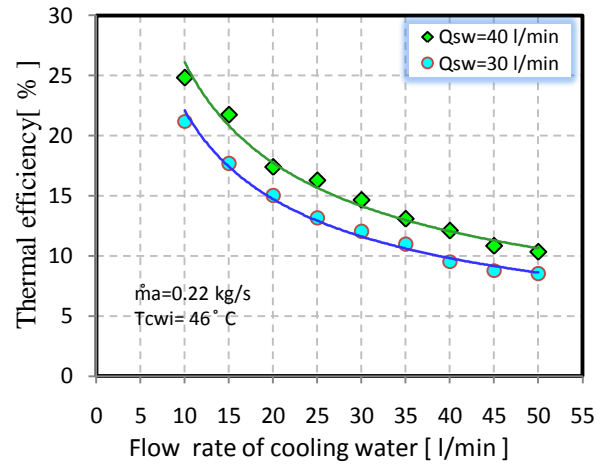


Fig. 12. Variation of thermal efficiency with cooling water flow rate for different spray water flow rates.

The effect of cooling water flow rate on exergy destruction for different spray water flow rates illustrated in Figure (13). As discussed in previous figure, when spray water flow rate increases exergy destruction decreases, whereas in this figure, it is state that the exergy destruction increases while cooling water flow rate increases due to increase in total water exergy. The exergy of cooling water depends mainly on the cooling water flow rate, so any increase in cooling water flow rate causes an increase in total exergy of water.

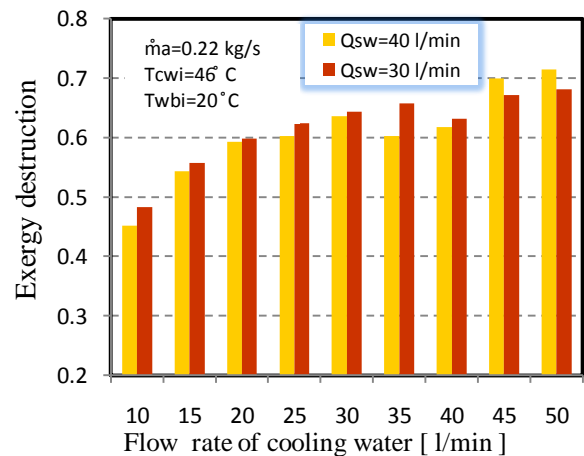


Fig. 13. Variation of exergy destruction with cooling water flow rate for different spray water flow rates.

The effect of cooling water flow rate on exergy efficiency for different spray water flow rates illustrated in Figure (14). From this figure, it can be seen that the exergy efficiency decreases when cooling water flow rate increased and spray water flow rate decreased.

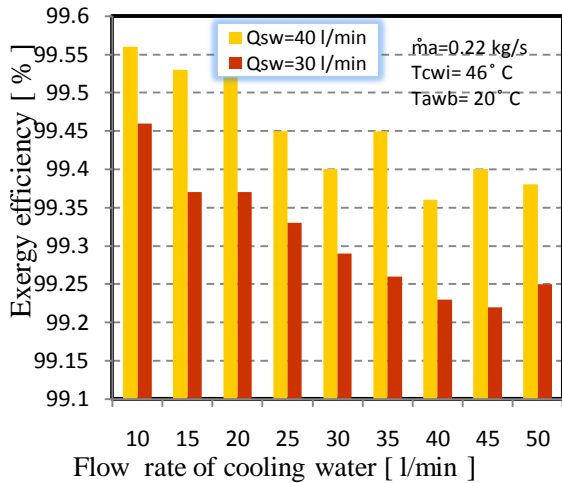


Fig. 14. Variation of exergy efficiency with cooling water flow rate for different spray water flow rates.

The relationship between the total exergy change of water and air with cooling water flow rate is illustrated in Figure (15). It could be clearly seen that the total exergy change of water and air are proportional to the cooling water flow rate. As expected, the total exergy change of water increases with the increases in cooling water flow rate as a result of increasing in exergy of cooling water. Also, it could be seen that the difference between total exergy change of water and air increases with increasing in cooling water flow rate.

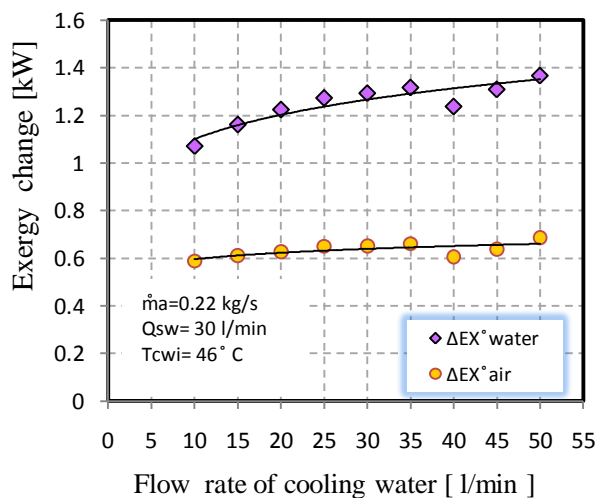


Fig. 15. Variation of total exergy change of water and air with cooling water flow.

3.3. Influence of Inlet Cooling Water Temperature

Cooling capacity with respect to variable inlet cooling water temperature and spray water flow rate has been shown in Figure (16). It is shown that if the spray water flow rate remains constant, cooling capacity increases rapidly with the increase of inlet cooling water temperature due to increase in rate of heat and mass transfer. This behaviour is determined by different experiments of authors Shim et. al. (2008), [4] and Yoo et. al. (2010), [16].

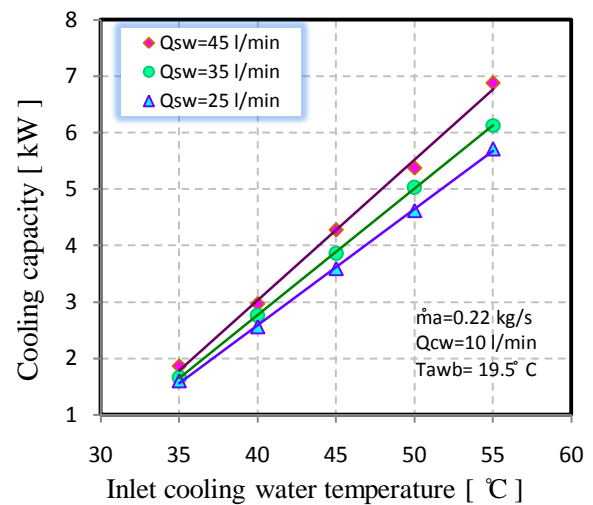


Fig. 16. Variation of cooling capacity with inlet cooling water temperature for different spray water flow rates.

Figure (17) indicate the effect of variable inlet cooling water temperature upon the tower thermal efficiency for different values of spray water flow rates. The thermal efficiency increases almost exponentially as the inlet cooling water temperature increases for all values of spray water flow rates. The thermal efficiency is high at higher inlet cooling water temperature and spray water flow rate. Small increment at low water temperature will gradually increases with an increase in water temperature.

Figure (18) depicts the effect of inlet cooling water temperature upon the overall exergy destruction for different values of spray water flow rates. As mentioned in Figure (8), for fixed inlet cooling water temperature, exergy destruction in inversely proportional to the spray water flow rate. On the other hand, from Figure (18), it was observed that by increasing inlet cooling water temperature, the exergy destruction increased due to increasing difference between

inlet water temperature and environmental air temperature which lead to increase thermal exergy of water. Also, increasing inlet water temperature causes an increase in the difference between the inlet and outlet cooling water temperature and thermal exergy of outlet cooling water increase too.

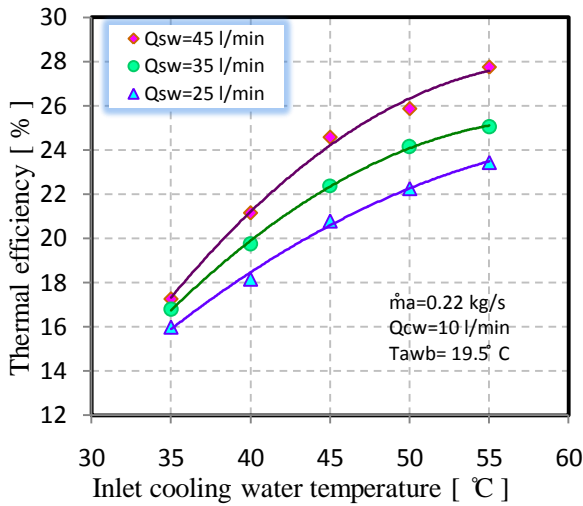


Fig. 17. Variation of thermal efficiency with inlet cooling water temperature for different spray water flow rates.

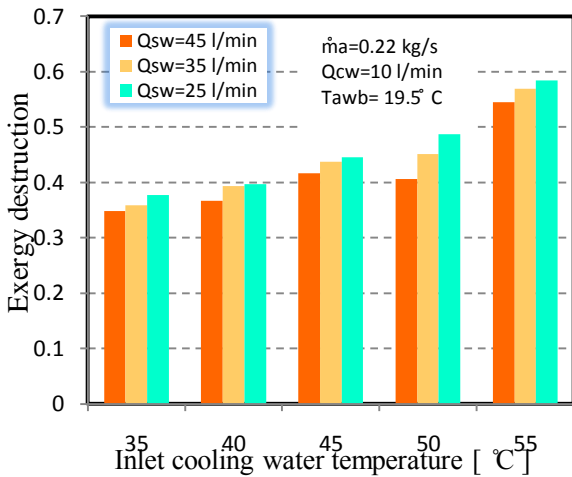


Fig. 18. Variation of exergy destruction with inlet cooling water temperature for different spray water flow rates.

The effect of cooling water flow rate on exergy efficiency for different spray water flow rates illustrated in Figure (19). The exergy efficiency decreases when cooling water flow rate increased and spray water flow rate decreased.

The variation of total exergy change of water and air with inlet cooling water temperature is

illustrated in Figure (20). It is indicated from this figure that the total exergy change of water and air increases exponentially with the increase of inlet cooling water temperature. As inlet cooling water temperature increases, inlet exergy of cooling, spray and makeup water increases lead to increase total exergy change of water. Also, it is shown that the difference between total exergy change of water and air increases with increasing in inlet cooling water temperature.

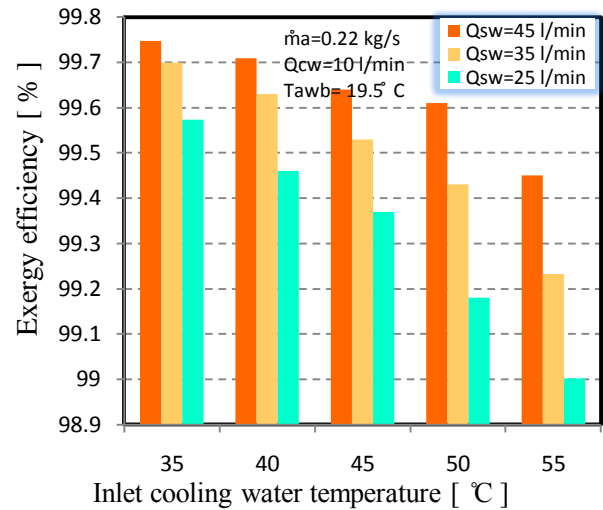


Fig. 19. Variation of exergy efficiency with inlet cooling water temperature for different spray.

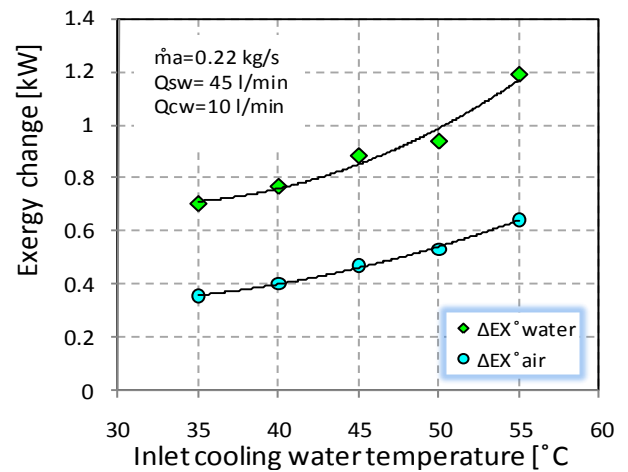


Fig. 20. Variation of total exergy change of water and air with inlet cooling water temperature.

3.4. Influence of Inlet AWBT

The change in cooling capacity versus inlet AWBT for different inlet cooling water temperature presented in Figure (21). It is clear that the cooling capacity is inversely proportional with the inlet AWBT for both inlet cooling water

temperatures. It is believed because any increase in inlet AWBT reflected to decreases the enthalpy potential between saturated vapour mixture (film surrounding the water droplet) and surrounding air. The effect of inlet AWBT on tower thermal efficiency for different inlet cooling water temperatures is investigated in Figure (22). It can be seen for both inlet cooling water temperatures that the thermal efficiency decreased as inlet AWBT increased which is brought about by the temperature fall at outlet of the heat exchanger. This behaviour was observed by Sarker (2007), [17]. Also, it can be apparent that higher tower thermal efficiency achieved at higher inlet cooling water temperature.

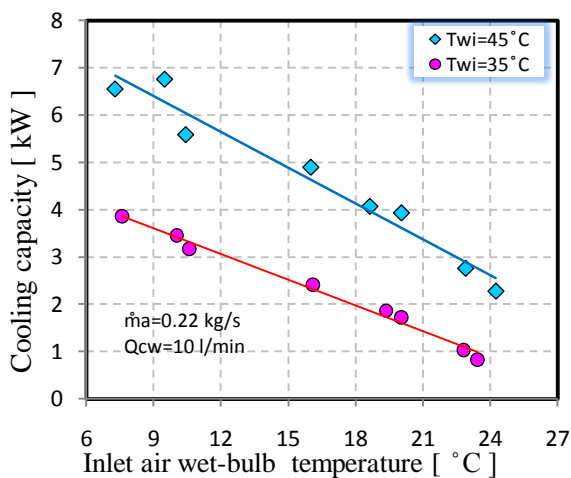


Fig. 21. Variation of cooling capacity with inlet AWBT for different inlet water temperatures.

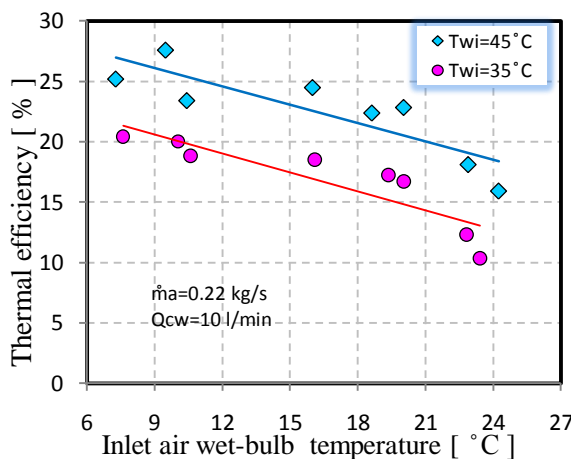


Fig. 22. Variation of thermal efficiency with inlet AWBT for different inlet water temperatures.

The effect of inlet AWBT on overall exergy destruction for different inlet cooling water temperatures is investigated in Figure (23). From this figure, it can be seen for both inlets cooling water temperatures that the exergy destruction depends strongly on the inlet AWBT. The increases in exergy destruction with the inlet AWBT correspond to an increasing in both rate of evaporation losses and dead temperature by increasing of AWBT.

The effect of inlet AWBT on tower exergy efficiency for different inlet cooling water temperatures is investigated in Figure (24). For each value of inlet cooling water temperature, as the inlet AWBT increased, the exergy efficiency is increased. Higher exergy efficiency achieved at lower AWBT and lower inlet cooling water temperature.

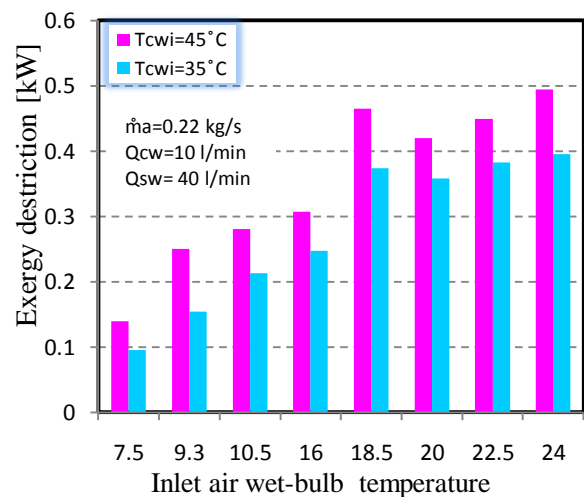


Fig. 23. Variation of exergy destruction with inlet AWBT for different inlet water temperatures.

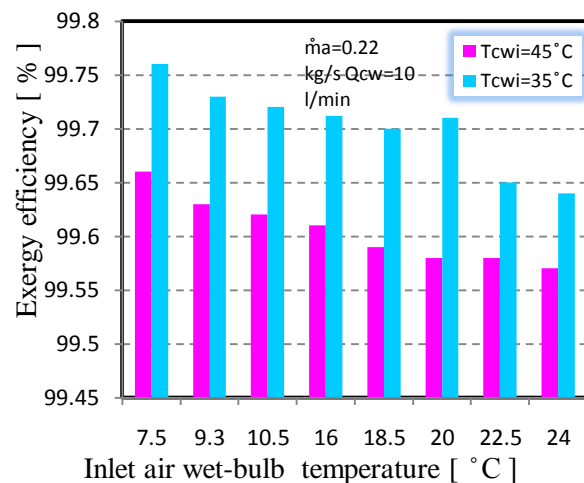


Fig. 24. Variation of exergy efficiency with inlet AWBT for different inlet water temperatures.

Effect of inlet AWBT on total exergy change of water and air is shown in Figure (25). The total exergy change of water is proportional to the inlet AWBT due to increase in exergy of makeup water caused by increases in evaporation losses, whereas, the total exergy of air increases with increase inlet AWBT before (19 ° C) then decreases with increase AWBT due to decreases in exergy of air via convection . Also, it is shown that the difference between total exergy change of water and air increases with increasing in inlet air wet bulb temperature.

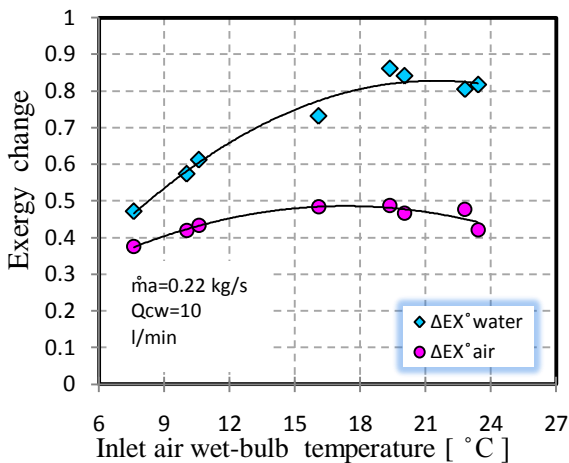


Fig. 25. Variation of total exergy change of water and air with inlet AWBT.

3.5. Influence of Added Packing

Figure (26) shows the cooling capacity comparing for different positions of packing. The result indicated that the cooling capacity for CWCT with packing lower under heat exchanger and CWCT with packing above heat exchanger approximately (28%) & (16%) higher than that CWCT respectively. In Figure (27), the thermal efficiency enhancement for different positions of packing is illustrated. It can be observed that the thermal efficiency for CWCT with packing lower under heat exchanger and CWCT with packing above heat exchanger approximately (52%) & (25%) higher than that CWCT respectively.

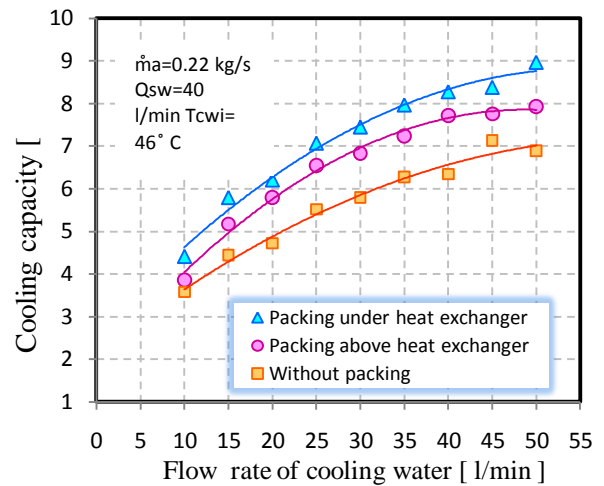


Fig. 26. Variation of cooling capacity with cooling water flow rate for different locations of packing.

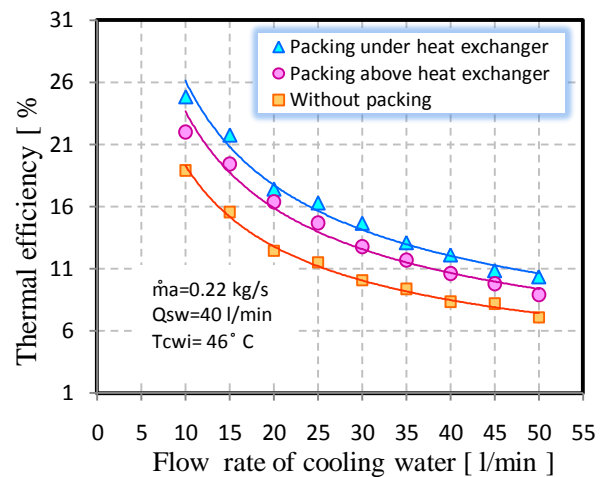


Fig. 27. Variation of thermal efficiency with cooling water flow rate for different locations of packing.

3.6. Empirical Correlations

According to the results of the experiments of this work, for different operational parameters, correlations for heat and mass transfer coefficients were developed for cooling tower operates without packing. These correlations are:

a-Mass transfer coefficient

$$\alpha_m = 0.000001(G_a)^{0.5038} (G_{sw})^{0.7456} (T_{cw})^{2.4478} \dots (19)$$

b-Heat transfer coefficient

$$\alpha_s = 0.1349(G_{sw})^{0.3758} (G_{cw})^{0.2051} (T_{cw})^{1.7749} \dots (20)$$

The average roots square mean error between correlations and experimental data for mass and heat transfer was (0.9666), (0.9424) respectively.

4. Conclusions

Thermal performance of CWCT with packing under heat exchanger was studied experimentally in view of energy and exergy analysis. The results can be summarized as follows:

1. Exergy destruction is directly proportional with air flow rate, cooling water flow rate, inlet cooling water flow rate and inlet AWBT whereas, it is inversely proportional with spray water flow rate. The behavior of exergy efficiency is completely opposite to the exergy destruction behavior.
2. Exergy change of water is greater than the exergy of air as a result of absorbing energy by water more than that by air because as the heating capacity of water is more and twice as much as that of the air. Also, exergy of air due to an evaporation more dominated function in the air exergy due to a convection.
3. 3-Cooling capacity increases when the air flow rate , spray water flow rate , cooling water flow rate and inlet cooling water temperature whereas, it decreases with an increase in AWBT. A comparison of the cooling capacity of the tower, it was found that the exergy destruction approximately less than 20%.
4. 4-The CWCT with packing has a better performance than without packing. Comparing CWCT with packing for both locations under and above heat exchanger, it has been observed that the best performance for the CWCT with packing under heat exchanger. Thermal efficiency for CWCT with packing under heat exchanger and CWCT with packing above heat exchanger approximately 40% and 25% higher than that CWCT without packing respectively

Nomenclature

A	total heat transfer area, m ²
C _p	specific heat at constant pressure, kJ/kg °C
CR	cooling range, °C
D	tube diameter, m
G	mass flux, kg/m ² .s
h	specific enthalpy, kJ/kg
k	thermal conductivity, W/m °C
\dot{E}_d	exergy destruction, kW
\dot{m}	mass flow rate, kg/s
q	cooling capacity, kW
Q	volume flow rate, l/min
Pr	Prandtl number
R	tube radius, m

R _a	individual gas constant for air, J/kg.K
R _v	individual gas constant for water vapor, J/kg.K
Re	Reynolds number
S	Specific entropy of saturated liquid water, J/kg.K
T	temperature, °C
U _o	overall heat transfer coefficient, W/m ² °C

Greek Symbols

α_m	mass transfer coefficient for water vapour, between spray water film and air, kg/m ² s
α_s	heat transfer coefficient between tube external surface and spray water film, W/m ² °C
α_c	heat transfer coefficient for water inside the tubes, W/m ² °C
η	thermal efficiency, %
η_{EX}	exergy efficiency, %
ρ	density, kg/m ³
Φ	relative humidity, %
ω	humidity ratio, kg/kg _{dry air}

Subscripts

a	air
cw	cooling water
in	inlet
o	dead state
out	outlet
sw	spray water
t	tube

References

- [1] Pascal Stabat, and Dominique Marchio. (2004). Simplified Model for Indirect-Contact Evaporative Cooling-Tower Behaviours. Applied Energy, Vol. 78, pp (433-451).
- [2] Armando C. Oliveira, and Jorge Facao. (2000). Thermal Behaviour of Closed Wet Cooling Towers for Use with Chilled Ceilings. Applied Thermal Engineering, Vol. 20, pp (1225-1236).
- [3] Bilal A. Qureshi and Syed M. Zubair. (2007). Second-law –Based Performance Evaluation of Cooling Towers and Evaporative Heat Exchangers. International Journal of Thermal Sciences, Vol. 46, pp (188-198).
- [4] Gyu-Jin Shim, M. M. A. Serker, Choon-Gun Moon, Ho-Saeng Lee, and Jung-In Yoon. (2008). Performance Characteristics of a Closed-Circuit Cooling Tower with Multi Path", World Academy of Science, Engineering and Technology, Vol. 2, pp (280-284).

- [5] Gyu-Jin Shim, M. M. A. Serker, Choon-Gun Moon, Ho-Saeng Lee, and Jung-In Yoon. (2010). Performance Characteristics of a Closed-Circuit Cooling Tower with Multiple Paths. *Heat Transfer Engineering*, Vol. 2, pp (992-997).
- [6] Heyns J. A., and Kroger D.G. (2010). Experimental Investigation into the Thermal-Flow Performance Characteristics of an Evaporative Cooler. *Applied Thermal Engineering*, Vol. 30, pp (492-498).
- [7] Zheng Wei-Ye, Dong-Sheng Zhu, Jin Song, Li-Ding Zeng and Hong-Jian Zhou. (2012). Experimental and Computational analysis of Thermal Performance of Oval Tube Closed Wet Cooling Tower. *Applied Thermal Engineering*, Vol. 35, pp (223-239).
- [8] Ramkumar Ramakrishnan and Aemugam Ragupathy. (2014). Thermal Performance Investigation of Mechanical Draft Cooling Tower Using Psychometric Gun Technique. *Heat transfer Engineering*, Vol. 35, pp (1344-1353).
- [9] Shah R.K and Sekulic P.D. (2003). *Fundamentals of Heat Exchanger Design*. John Wiley & Sons. Inc.
- [10] Yingghan Li, You Xinkui, Qiu Qi and Jiezhi Li. (2011). The study on the Evaporation Cooling Efficiency and Effectiveness of Cooling Tower of Film Type. *Energy Conservation and Management*, Vol. 52, pp (53-59).
- [11] Armando Oliveira, and Jorge Facao. (2008). Heat and Mass Transfer in an Indirect Contact Cooling Tower: CFD Simulation and Experiment. *Numerical Heat Transfer, Part A*, Vol. 54, pp (933-944).
- [12] Hasan A., and Sirén K. (2002). Theoretical And Computational Analysis of Closed Wet Cooling Towers And Its Application In Cooling Of Buildings. *Energy And Buildings*, Vol. 34, pp (477 - 486).
- [13] Incropera F.P , Dewitt D.P, Bergman T.L & Lavine A.S. (2011). *Fundamentals of Heat and Mass Transfer*. 7th ed., J. Wiley and Sons, New York.
- [14] Bejan Aarian. (1997). *Advanced Engineering Thermodynamics*. 2nd ed., J. Wiley, Singapore.
- [15] Bilal A.Qureshi and Syed M.Zubair. (2007). Second-law –based performance evaluation of cooling towers and evaporative heat exchangers. *International Journal of Thermal Sciences*, Vol. 46, pp (188-198).
- [16] Yoo Seong-Yeon, Jin-Hyuck Kim, and Kyu-Hyun Han. (2010). Thermal performance analysis of heat exchanger for closed wet cooling tower using heat and mass transfer analogy. *Journal of Mechanical Science and Technology*, Vol.24, No.4, pp (893-898).
- [17] Sarker M. M. (2007). Investigation on the Optimum Design of Heat Exchangers in a Hybrid Closed Circuit Cooling Tower. *Journal of Mechanical Engineering*, Vol. 37, pp (52-57).

تحليل الطاقة والطاقة المتاحة على برج تبريد رطب مغلق مطور في العراق

قاسم صالح مهدي* حيدر محمد جفال**

*قسم الهندسة الميكانيكية/ كلية الهندسة/ الجامعة المستنصرية

**قسم هندسة البيئة/ كلية الهندسة/ الجامعة المستنصرية

*البريد الإلكتروني: qasim602006@yahoo.com**البريد الإلكتروني: hayder.jaffal@yahoo.com

الخلاصة

تتضمن هذه الدراسة تحليلاً عملياً لهرج تبريد رطب مغلق مطور على فق قانوني الديناميك الحرارية الأول والثاني من أجل زيادة المعرفة في هذا الحقل الهندسي المهم في العراق. لهذا الغرض صمم وصنع واختبر نموذج مطور لبرج تبريد مغلق رطب بإضافة حشوات لسعة تبريد (٩ كيلو واط). أجريت التجارب لتوضيح تأثيرات المعاملات التشغيلية والتصميمية على الأداء الحراري للبرج. في مقطع الاختبار ودرجة حرارة ماء الرش وكل من درجة الحرارة الجافة والرطوبة النسبية للهواء التي تم قياسها في نقاط متوسطة للمبادل الحراري والحشوة. الطاقة المتاحة للماء والهواء تم حسابها بتطبيق طريقة تحطيم الطاقة المتاحة على برج التبريد. إن النتائج التجريبية وضحت تحسناً ملموساً للأداء الحراري عند إضافة الحشوة إلى البرج المغلق. وتم ملاحظة الأداء الأفضل عند إضافة الحشوة أسفل المبادل الحراري على الرغم من كبر ضياع الطاقة المتاحة لهذه الحالة. وجد أن الكفاءة الحرارية عند إضافة الحشوة أسفل وأعلى المبادل الحراري بأفضلية تصل إلى نسبة ٤٠% و ٢٥% مقارنة مع برج التبريد المغلق بدون إضافة الحشوة على التوالي. لوحظ كذلك أن الطاقة المتاحة المحطمة تتناسب تناسباً مباشراً مع تدفق الهواء تدفق ماء التبريد، درجة حرارة الهطول لماء التبريد ودرجة حرارة الهواء الرطبة الداخلة للهواء بينما تتناسب تناسباً عكسياً مع معدل تدفق ماء الرش. سلوك كفاء الطاقة المتاحة معاكس لسلوك ضياع الطاقة المتاحة. بالمقارنة مع سعة التبريد للبرج ووجد أن الطاقة المتاحة المحطمة تشكل نسبة اقل من ٢٠%. تم استنتاج عدد من العلاقات التجريبية للتنبؤ بمعامل انتقال الحرارة والكتلة بدلالة المتغيرات التشغيلية.